Biomaterials Science

Precise Patterning of SEBS Surface with UV Lithograph to Evaluate Platelet Function through Single Platelet Adhesion

Journal:	*Biomaterials Science*
Manuscript ID:	BM-ART-03-2014-000072.R1
Article Type:	Paper
Date Submitted by the Author:	03-Apr-2014

Complete List of Authors:	Ye, Wei; Changchun Institute of Applied Chemistry,Chinese Academy of Sciences, Shi, Qiang; Changchun Institute of Applied Chemistry, Chinese Academy of Sciences, Wong, Shing-Chung; Department of Mechanical Engineering, University of Akron,, Hou, Jianwen; Changchun Institute of Applied Chemistry,Chinese Academy of Sciences, Fan, Qungfu; Polymer Materials Research Center and Key Laboratory of Superlight Materials and Surface Technology, Ministry of Education, College of Materials Science and Chemical Engineering, Harbin Engineering University,, Xu, Xiaodong; Harbin Engineering University, College of Materials Science and Chemical Engineering Yin, Jinghua; Changchun Institute of Applied Chemistry,Chinese Academy of Sciences,

Graphical Abstract

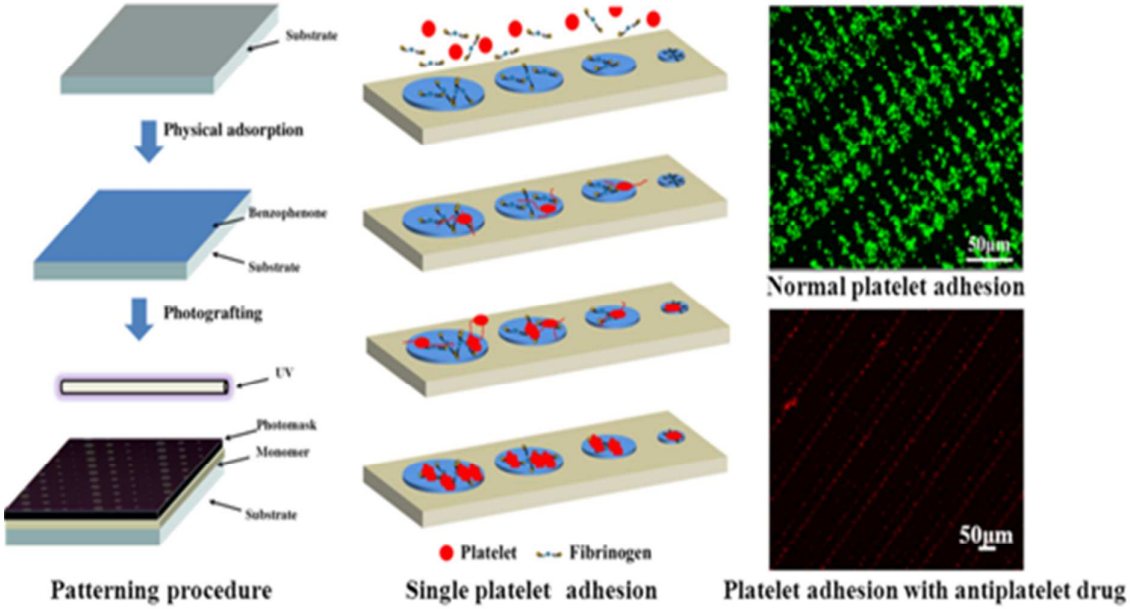

We reported a generally applicable UV lithography technique with a photomask, which achieved stable, physical adhesive sites in the range from 12 μm to 3 μm on SEBS surface. Single platelet adhesion on the patterned surface was in a controlled manner and quantitatively probed. Patterned surface also rendered adhesion sensitive to adhesive proteins and assessed platelet function in the presence antiplatelet agents through single platelet adhesion. The methodology has the potential to enable a rapid, accurate point-of-care platform suitable to evaluation of platelet function, detection of dysfunctional platelets and the administration of antiplatelet agents.

Biomaterials Science

RSCPublishing

ARTICLE

Precise Patterning of SEBS Surface with UV Lithograph to Evaluate Platelet Function through Single Platelet Adhesion

Cite this: DOI: 10.1039/x0xx00000x

Received 00th January 2012,
Accepted 00th January 2012

DOI: 10.1039/x0xx00000x

www.rsc.org/

Wei Ye,[a] Qiang Shi,*[a] Shing-Chung Wong,[b] Jianwen Hou,[a] Xiaodong Xu[c] and Jinghua Yin*[a]

Platelets have exhibited capabilities beyond clotting in recent years. Most of their functions are related to the nature of platelet adhesion. Establishing a facile method to understand the platelet adhesion and assess the platelet function through mechanism and mechanics of adhesion becomes highly desired. Here, we reported a generally applicable UV lithography technique with a photomask, which performs selective surface functionalization on large substrate areas, for achieving stable, physical adhesive sites in the range from 12 μm to 3 μm. Our study demonstrated that the patterned surface facilitated probing single platelet adhesion in a quantitative manner, and rendered platelets sensitive to adhesive proteins even at a low protein concentration. In addition, the platelet function in the presence of antiplatelet (anticancer) agents on platelet could be accurately estimated based on single platelet adhesion (SPA). This work paves new way to understand and assess blood platelet function. The SPA assay methodology has the potential to enable a rapid, accurate point of care platform suitable to evaluation of platelet function, detection of dysfunctional platelets, and assay of drug effects on platelets in cancer patients.

1. Introduction

Platelets have exhibited capabilities no one imagined they had in recent years.[1] These small anucleate cells that circulate in the blood of mammals are not only critical effectors of hemostasis, blood clotting and wound repair but defenders against microbes[2] and engineers to shape the vascular system in new borns. Yet for all their benefits, platelets can lodge in blood vessels, depriving tissue of oxygen and instigating a stroke and heart attack, in addition, they can foster cancer, rheumatoid arthritis, and other diseases.[3] A platelet biochemical defect,[4] poor platelet quality[5] or the presence of antiplatelet agents[6,7] can reduce or abolish platelet function. Understanding the mechanisms that drive platelet function and assessing the platelet function effectively are therefore important in both scientific and clinical areas. Platelets are highly adhesive in nature and almost all functions of blood platelets are related to platelet adhesive properties.[7-13] It is our goal to quantitatively understand and evaluate platelet functions through single platelet adhesion on substrates.

Micropatterning provides a powerful tool to create and model cues on soft materials, which define the microenvironment of platelet in spatially confined areas.[8,9] A common approach is to create a passive surface and then introduce a pattern of protein on the substrate which allows platelets to adhere to the pattern according to their natural preferences.[14] Polymers, such as polyethylene glycol (PEG) and polymer of 2-methacryloyloxyethyl phosphorylcholine (MPC), and bioactive ligands, such as, fibrinogen and some related synthetic peptides are used extensively.[14-19] However, evaluation of platelet function on micropatterned surface is not successful due to multiple steps for surface patterning and failure to probe adhesive behavior in a quantitative manner.[8,15] In addition, the influences of microenvironmental geometry on the platelet function are often misinterpreted when patterned proteins are used to control platelet adhesion.[17] Therefore, development of facile method to pattern surface, which can control single platelet adhesion with the guidance of physical properties and evaluate the platelet function in a quantitative manner, will facilitate establishing adhesion-function relationship of platelets and find potential applications in

clinical diagnostics of platelet-related disease and point-of-care testing.[18-20]

Here we present a simple method for surface patterning with conventional UV illumination and a photomask to create stable and physical adhesive sites with diameter from 12 μm to 3 μm over large area. Our strategy is based on a controlled polymerization of MPC on the whole surface of substrate and degradation of obtained polymer of MPC at UV-exposed domains (adhesive sites) with UV irradiation in one step.[15] Styrene-b-(ethylene-co-butylene)-b-Styrene elastomer (SEBS) is used for substrate due to its unique nanostructures, good biocompatibility and outstanding stability under physiological conditions.[21] The single platelet adhesion on patterned surface is studied in a quantitative manner and platelet function in the presence of antiplatelet (anti-cancer) agents is accurately evaluated based on single platelet adhesion assay. We demonstrate that single platelet adhesion on the patterned surface occurs in a controlled manner following the steps of (i) initiation, (ii) spreading and (iii) stabilization. The initiation is a rate-determined step under a confined environment. Patterned surfaces make adhesion sensitive to adhesive proteins and enable assessment of platelet function through single platelet adhesion. Our work paves a new way to understand and evaluate the platelet function both in research and clinical diagnostics. The single platelet adhesion assay methodology has the potential to enable a rapid, accurate point-of-care platform suitable to evaluation of platelet function, detection of dysfunctional platelets and the administration of antiplatelet agents.

2. Materials and methods

2.1 Chemicals and Materials

SEBS copolymer with 29wt% styrene (Kraton G 1652) was purchased from Shell Chemicals. Benzophenone (BP) was supplied by Peking Ruichen Chemical (China). 2-Methacryloyloxyethyl phosphorylcholine (MPC) was purchased from Nanjing Letianran Science and Technology Research Center, China. Fluorescein isothiocyanate-labeled bovine serum fibrinogen (BFg) and Fluoresce in isothiocyanate labeled phalloidine were purchased from Sigma-Aldrich. Phosphate-buffered saline (PBS 0.9% NaCl, 0.01M phosphate buffer, pH 7.4) used for platelet adhesion experiment was prepared freshly. ABT-737 was purchased from Selleck Chemicals. Other reagents were AR grade and used without further purification.

2.2 Preparation of SEBS films

SEBS was dissolved in xylene to form 15 % (w/w) solutions and poured onto a clean glass. After the solvent evaporated, a smooth SEBS films (0.2 mm thick) was obtained. The SEBS films were cut into strips of 2 cm ×1.5 cm and ultrasonically washed with deionized water and ethanol for 30 min, and then put in a vacuum oven for 24h to dry.

2.3 Surface micro-patterning

The SEBS films were immersed in the ethanol solution of BP (1.5 wt%) for 30min and dried at room temperature. Then the film was put on the quartz plate (3mm thick) and coated with 5 wt% aqueous solution of MPC; the pre-designed chrome photo-mask was put on the SEBS surface directly. Then the sandwiched system (shown in Fig. 1a) was exposed to UV light (high-pressure mercury lamp, 400W, main wavelength 380nm) for 10min. All the films were washed with deionized water and ethanol to remove residual monomer, followed by drying in a vacuum oven for at least 24h.

2.4 Platelet adhesion assay

Fresh blood collected from a healthy rabbit was immediately mixed with 3.8 wt% sodium citrate solution at a dilution ratio of 9:1. (The experiments were carried out in accordance with the guidelines issued by the Ethical Committee of the Chinese Academy of Sciences.) Platelet rich plasma (PRP) was obtained from the supernatant after centrifugation of whole blood at 1000 rpm for 15 min. The SEBS films were immersed in PBS (pH 7.4) at 37 °C for 2 h to equilibrate the surfaces. Then PRP was deposited onto each sample and allowed to adhere for a given time at 37 °C. The non-adherent platelets were rinsed away by PBS for several times. The samples were fixed with a freshly prepared solution of 2.5 wt% glutaraldehyde in PBS at 37 °C for at least 2 h. After rinsing with PBS, the adherent platelets were dehydrated in ascending ethanol/water mixtures (10, 30, 50, 70, 90 and 100 %) for 30 min in each step, dried under vacuum and finally sputter coated by gold. Platelet adhesion was characterized by a field-emission scanning electron microscopy (SEM, Sirion-100, FEI, USA). Platelets were stained for F-actin with Fluorescein isothiocyanate labeled phalloidine, and then characterized by confocal laser scanning microscope (Zeiss LSM 710 confocal microscope).

2.5 Protein adsorption

Fluoresce in isothiocyanate-labeled bovine serum fibrinogen (FITC-labeled BFg) was dissolved in PBS (pH 7.4) at concentration of 0.1 mg/ml. Then BFg was deposited onto each sample and incubated for 1.5 h at room temperature in a dark environment to allow fibrinogen to adsorb onto the virgin and patterned SEBS surface. Following protein incubation, the films were rinsed with PBS and deionized water to remove any weakly adsorbed protein. Fibrinogen, fibronectin and collagen (Rat tail tendon collagen type I) were pre-adsorbed onto patterned SEBS films at a concentration of 0.1 mg/ml. Washed rabbit platelets with the concentration of 2×10^6/ml were seeded on the pre-adsorbed protein films at room temperature for 15min, 20min, 30min, 60min and 90min, respectively. After fixed by 2.5 wt% glutaraldehyde and dehydrated in ascending ethanol/water mixtures, platelet was visualized by a field-emission scanning electron microscopy (FSEM).

2.6 Anti-cancer agents

Bcl-2 homology 3 (BH3) proteins play an important role in inducing apoptosis by inhabiting the function of Bcl-2 family proteins. In the experiment of patterned SEBS surface, ABT-737 as a typical BH3 mimetic was added to platelet rich plasma (PRP). ABT-737 solution (100 μg/ml in DMSO) was diluted to 1.5, 3, 6 μg/ml in PBS. PRP was pretreated for 1 or 2 hours at 37°C with ABT-737. The platelet adhesion assay was performed as the procedure described above.

2.7 Statistics

The analysis involved both counting of adhered platelets (~0.01mm^2 per SEM image) and the analysis of platelet morphology by using free software Image-J. The data from multiple separate experiments were analyzed and reported as the mean ± the standard error (SE) of the mean. The data were analyzed by one-way ANOVA method, the statistical significance was accepted when $p< 0.05$.

3 Result and discussion

3.1 Fabrication of patterned SEBS surface

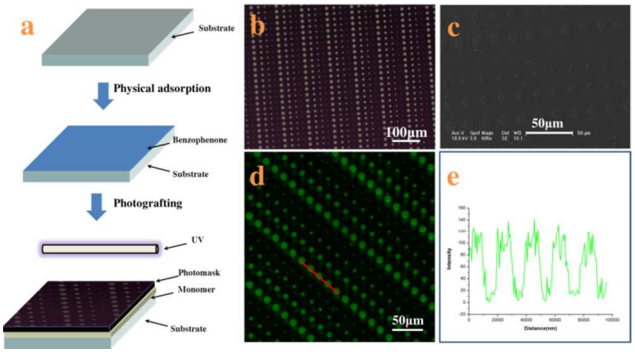

Fig. 1 Process for surface patterning and texture of patterned surface. (a) The process to pattern the surface of SEBS; (b) optical microscope image of structure of a photomask; (c) SEM image of patterned surface; (d) fluorescent image of FITC-labeled fibrinogens adsorbed on the patterned surface; (e) line intensity of fluorescent scan. These images demonstrate that the uniform and fine adhesive sites on patterned structure are achieved by controlled UV-polymerization of MPC and degradation of PMPC at selected area through a photomask.

Micropatterned surfaces of SEBS are fabricated by UV illumination with a photomask. The process to pattern the surface of SEBS is shown in Fig. 1a. The SEBS films firstly adsorb benzophenone (BP) physically, followed by coating with MPC aqueous solution; then the photomask is put on the SEBS surface directly and irradiated by UV for 10 min. Based on grafting polymerization of MPC on whole surface of SEBS and subsequent degradation of PMPC on UV-exposed domains through the photomask, platelet adhesive sites are created on these areas, while UV-unexposed domains are hydrophilic and resist platelet adhesion.[15] The resultant micro-patterned surface is characterized by a SEM. Fig. 1c shows that the structure of photomask (Fig. 1b) is well duplicated on the SEBS surface. The array of adhesive sites is clearly observed and the diameters of adhesive sites are approximately 12, 9, 6, 3 μm, respectively. As the adhesive sites are more hydrophobic than other place on the patterned surface, BFg can be easily adsorbed at the adhesive sites and are used to further characterize the structure of SEBS surface.[22] Fig. 1d shows the fluorescent image of BFg adsorbed on the patterned surface, the array of blue spots indicates the perfect structure of adhesive sites. The line intensity of fluorescent scan (Fig. 1f) confirms the space between the adhesive sites is in a well-controlled manner.[23] These results demonstrate that this method can achieve the uniform and fine adhesive sites on patterned structure.

Obviously, the patterned surface fabricated in this way has many advantages for studying platelet adhesion and evaluating its function: i) it provides an unique platform to probe single platelet adhesion induced by physical properties of surface; ii) the size of adhesive sites range from 12 μm to 3 μm, which enable quantitatively investigating the single platelet adhesive behavior, platelet-substrate and platelet-platelet interaction under a confined microenvironment; iii) the platelet function can be accurately assessed based on single platelet adhesion assay.

3.2 Single platelet adhesion on patterned surface

To probe adhesive behavior of single platelet on the patterned SEBS substrate, PRP are incubated on the patterned surface for a specific time at 37°C, then fixed by 2.5 wt% glutaraldehyde. The SEM images of platelet adhesion on the patterned surface of SEBS are shown in Fig. 2.

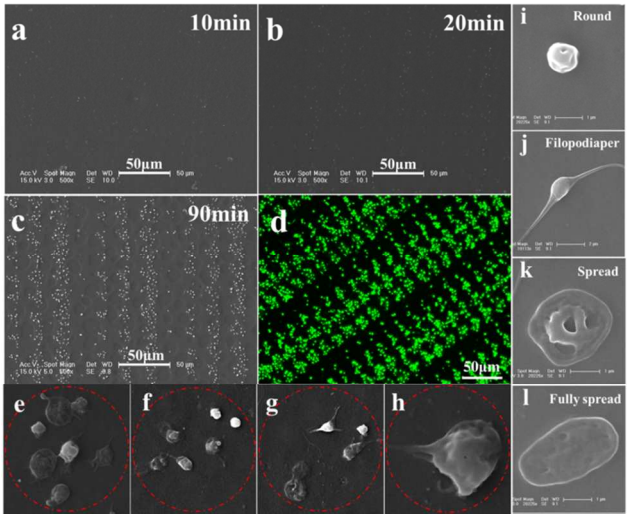

Fig.2 Time-dependent platelet adhesion and morphology of adherent platelet. (a)-(c) platelet adhesion on the patterned surface after 10 min, 20 min and 90 min incubation, respectively; (d) fluorescent image of array of adherent platelets; (e)-(h) number and morphology of adherent platelets at 12, 9, 6, 3μm adhesive sites, respectively. (i-l) the adherent platelets with the shape of round, filopodiaper, spread and fully spread, respectively. The patterned surfaces enable investigating the single platelet adhesive behavior, platelet-substrate and platelet-platelet interaction under confined microenvironment.

The lack of hydrophilicity renders the platelets adherent and spread selectively on adhesive sites.[15,18] After 10 min incubation, only a few single platelet attach onto the 9 and 12 μm adhesive sites, while no adherent platelets is observed on 6

and 3 μm adhesive sites (Fig. 2a). After 20 min incubation, some adherent platelets appear at 6 and 3 μm adhesive sites (Fig. 2b). After 30 min incubation, more platelets adhere to the adhesive sites and the array of adherent platelets comes to emerge (Fig. 2c). The array of platelets at 120 min is clearly observed by confocal lasers scanning microscope (Fig. 2d). Fig. 2e-2h shows the morphology of adherent platelets at varied adhesive sites. The round shape is dominant at 3 μm sites, round shape, filopodiaper and fully spread are found at 6, 9 and 12 μm adhesive sites, respectively. The fully spread of adherent platelet is in high ratio at 12 μm adhesive sites. The morphology change is controlled by actin polymerization of platelet.[13] The limited space may inhibit the polymerization of actin, resulting in round shape at 3 μm adhesive sites. On the contrary, relatively large room allows the polymerization of actin to form filopodiaper and fully spread at 12 μm adhesive sites, as a result, fully spread is dominant at 12 μm adhesive sites. The round shape of platelet appearing at the adhesive sites indicates these platelets remain inactive, which is in agreement with the results observed by Ruggeri *et al*.[24] In addition, the size of adhesive sites determines the maximal number of adherent platelets. For example, 1 adherent platelet in 3 μm adhesive sites, 2-3 platelets in 6 μm sites, 4-5 in 9 μm sites, and 5-6 platelets in 12 μm sites. The morphology and number of platelets at varied adhesive sites indicate the geometric confinement on platelet adhesion.

Based on the SEM picture, the time dependent of platelet adhesion is plotted in Fig. 3a. The adhesive behaviours are different at varied adhesive sites. The average number (AN) of platelets at 3 μm sites increases linearly with time from 0.2 at 10 min to nearly 1 at 90 min. The AN of platelet adherent at 6, 9 and 12 μm first increases with incubation time, then reaches the plateau at 90 min and does not increase any more, exhibiting three stages including the initiation, extension and stabilization (or termination) of adhesion, in agreement with well-established mechanism of platelet adhesion and activation.[10]

Interestingly, acceleration occurs in the extension stage of platelets adherent at 6, 9 and 12 μm sites after 30 min incubation, showing the platelet-platelet interactions speed up the adhesion process. After reaching the maximal number of adherent platelets, no more platelets can attach to the adhesive sites, indicating the termination of adhesion is controlled by the size of adhesive sites.[25] This is a very important function for normal platelets, since the extent of the platelet response to injury is subject to tight regulation.[12] Appropriate platelet activation limits the extent of blood loss following vascular injury and promotes subsequent wound healing without causing vascular occlusion.[26] This work shows that geometric confinement may be one factor to control the termination of thrombus. The time evolution of morphology for adherent platelet at 12 μm and 3 μm adhesive sites are shown in Fig. 3b and 3c, respectively. At 12 μm adhesive sites, the attached platelets are in fully spreading shape after 15-20 min incubation, and then some platelets extend with filopodiaper, resulting in high ratio of filopodiaper shape. As newly adherent platelets become stable with fully spreading shape, the fully spreading shape is dominant again at 90 min incubation (Fig. 3c).

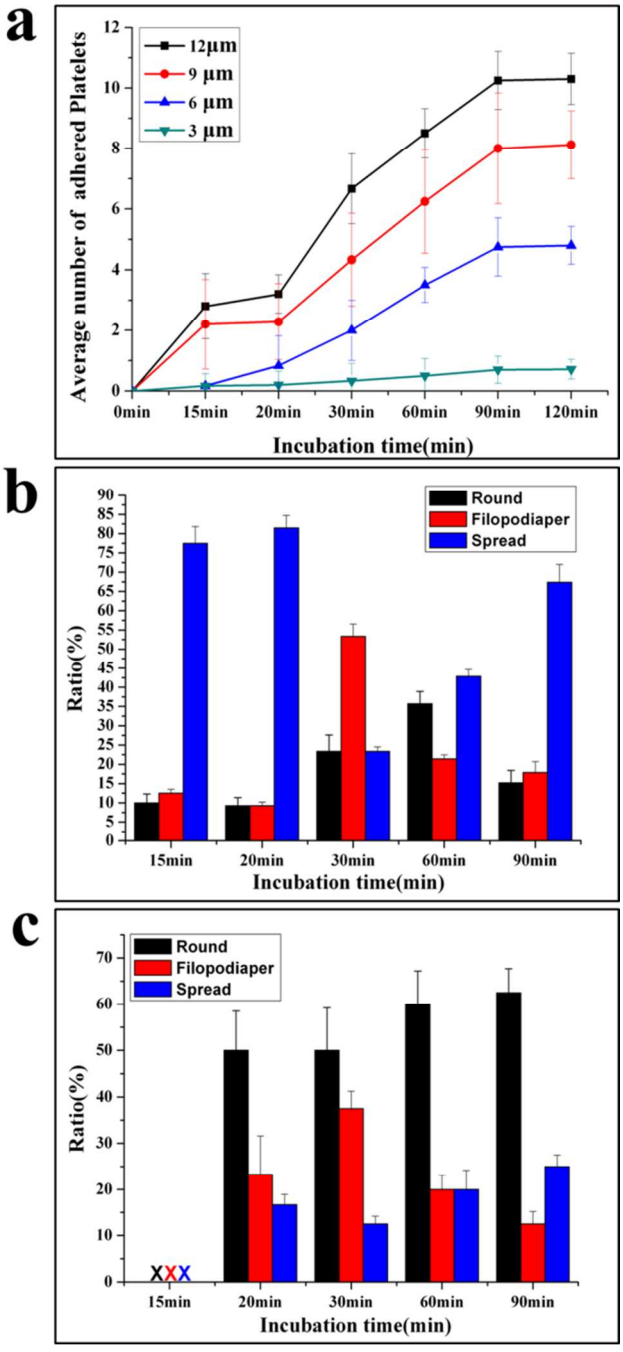

Fig.3 Time-dependent adhesion and morphology of adherent platelets. (a) time dependent of platelet adhesion; (b) time evolution of morphology of adherent platelets at 12 μm adhesive sites; (c) time evolution of morphology of adherent platelets at 3μm adhesive sites. The patterned surfaces facilitated investigating platelet adhesive behavior in a quantitative manner. Initiation of adhesion is a rate-determined step.

At 3 μm adhesive sites, no platelets are detected after 15 min incubation; few platelets with round shape appear at 20 min. Then some adherent platelets begin to form filopodiaper,

lowering the ratio of round shape. But round shape is dominant until 90 min incubation (Fig. 3b).

The morphology change shows the importance of stable adhesion of single platelet to initiate the adhesion.[27]The platelets first attach at adhesive sites and need to stabilize their adhesion by increase adhesive forces. For the platelets at 12 μm adhesive sites, they can form protrusions and then contract into more compact structure (fully spread) to increase the attachment area, but at 3 μm adhesive sites, platelets cannot extend and contract due to limited space, they stabilize the adhesion only by increasing the attachment time.[28] Thus, after 15 min incubation, platelets adhere at 12 μm adhesive sites with fully spread, while after 20 min incubation, platelets appear at 3 μm adhesive sites with a round shape. The morphology change of adherent platelets at 3 and 12 μm adhesive sites confirms the three-stage adhesion under the confinement[10] and the initiation of adhesion is the rate-determined step for the adhesive process.

Table 1. Adhesion rate, morphology and number of PRP on patterned surface

Adhesive sites	Adhesion rate number/min		The ratio of fully spread /%	Maximum number of platelets
	V_0 (initial rate)	V_s (rate of spread)		
3μm	0.02	0.01	25	0.7±0.4
6μm	0.04	0.12	30	4.8±1
9μm	0.12	0.20	48	8.0±1.8
12μm	0.16	0.37	70	10.2±1

The patterned surfaces facilitate probing platelet adhesive behaviour in a quantitative manner. The data for adhesion induced by physical properties are listed in Table 1. Table 1 shows that initial rate of adhesion (the slope of adhesion curve before 15 min incubation), rate of spread (average rate from 15 min to 90 min), ratio of fully spread and maximal number of adherent platelets are proportional to the size of adhesive sites. Initial rate is slower than spreading rate at each adhesive site, confirming that initiation is a rate-determined step under the confined environment. The data for adhesion at 3 μm and 12 μm adhesive sites are especially useful to shed light on the feature of adhesion. 3 μm adhesive site is comparable to the size of single platelet, geometric confinements make it difficult for platelets to approach and attach onto this site, and only the most active platelets can reach and form the stable adhesion at 3μm adhesive sites through receptor-ligand reaction. The initial adhesive rate is a good indicator to assess the activity of platelets and reactivity of platelet and substrate.[8] For 12 μm adhesive site, the number of platelets initially attach on the adhesive site is more than other sites, and these adherent platelets can release a number of biological active substances and extend into the filopodiaper to induce adjacent platelet adhesion, resulting in the acceleration of adhesive process.[7] Therefore, the rate at acceleration, shape change and maximal number of adherent platelets at 12 μm adhesive sites are indicators for platelet activation and platelet-platelet interaction.[28] The data of adhesion at 3 and 12 μm adhesive sites provide the standard to evaluate the platelet function.

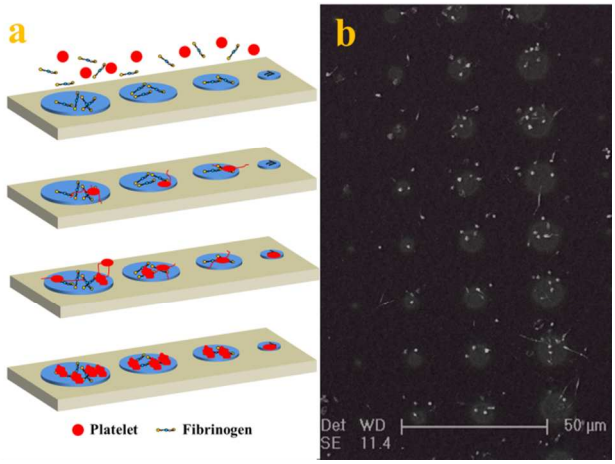

Fig.4 Mechanism of single platelet adhesion on the patterned surface (a) and SEM images of adherent platelets on patterned surface after 60 min incubation (b) The adhesion is in the controlled manner following three stages of initiation, extension and stabilization.

With the adhesive behaviour and morphology change of adherent platelets, the mechanism of platelet adhesion and activation on the patterned surface is tentatively proposed (shown in Fig. 4a). Because PRP usually contains about 2-3 mg/ml fibrinogen,[29] when PRP contacts with the patterned surface, the fibrinogen first adsorbs to the adhesive sites to mediate the platelet adhesive behaviours by binding with receptor on platelet membrane and arrests the platelets to the adhesive sites.[30] Platelets preferentially attach at adhesive sites with large adhesive sites, but need a long time to adhere at small adhesive sites due to the confinement. The adherent platelets become stable and release a number of biological active substances upon activation such as α-granules which contained vWF, coagulation factor V, and fibronectin to induce adjacent platelet adhesion, resulting in the acceleration of adhesive process.[7] At the same time, some platelets begin to form pseudopodia to probe and sense the geometry of their microenvironment, inducing adjacent platelets to the adhesive sites.[31] Intracellular signalling downstream of agonist receptors activates integrin $\alpha_{IIb}\beta_3$ (GPIIb/IIIa), making cohesive interactions between platelets possible. The platelets not only use the protrusions to enable more physical connections with other platelets at the adhesive sites but using their action-myosin interactions to pull the adherent platelets into a more compact structure (fully spread).[32] The number and morphology of adherent platelets at final stage depend on the surface properties and the size of adhesive sites. The mechanism of platelet adhesion under confined environment is confirmed by

the morphology of adhesion on the patterned surface after 90 min incubation (Fig. 4b). It has been proposed that in the process, platelets not only provide a surface that can facilitate leukocyte immigration into surrounding tissue but also serve as a source of inflammatory mediator and molecules that promote wound healing.[1] Although platelet adhesion to the injure sites is thought to be spatial and temporal,[10] platelet adhesion to the adhesive sites tends to happen orderly on series of events. This difference may be due to the low concentration of platelets used in the experiment[28] and confinement on the patterned surface.[25, 27] The controlled platelet adhesion facilitates studying the characteristic of adhesive behaviours to evaluate platelet function.

3.3 Sensitivity of single platelet adhesion to adhesive proteins

The sensitivity of platelet adhesive behaviour to adhesive proteins is a key standard to evaluate the accuracy of patterned surface in assessing the platelet function.[33-36] Fibrinogen, fibronectin and collagen are pre-adsorbed at adhesive sites to induce the platelet adhesion. Fibrinogen is the major plasma protein, which is made up of three globular units connected by two rods. Its γ chain C-terminal dodecapeptide is the most important site in mediating platelet adhesion and aggregation. Fibronectin is present in plasma, the subendothelium of the vessel wall, and the α granules of platelets. It has the similar binding sites with fibrinogen to the glycoprotein (GP) IIb-IIIa receptor ($\alpha_{IIb}\beta_3$) on the membrane of platelets.[34] Collagens are among the major constituents that determine the thrombogenicity of the vessel wall. The interaction of collagen with platelets membrane GP Ia-IIa and GPVI is in an important step in their adhesion to the subendothelium.[35] All the three proteins contribute to the platelet adhesion and aggregation on the substrate, but fibrinogen and fibronectin tend to support both platelet-surface and platelet-platelet interactions,[6, 34] while collagen show the tendency to stabilize the adhesion.[36]

Fig. 5 shows the SEM images adhesion of washed PRP on the patterned surface with adhesive proteins pre-adsorption after 60 min incubation. To decrease the effect of fibrinogen in plasma on adhesion, the PRP is washed with PBS, as a result, the concentration of fibrinogen is decreased by 92.8±0.3% (Support Information). The density of adsorbed proteins on adhesive site is measured by bicinchoninic acid (BCA) protein assay. The amount of fibrinogen, fibronectin, and collagen adsorbed are 6.83±0.30 μg/cm^2, 4.38±0.18 μg/cm^2, 1.09±0.02 μg/cm^2, respectively, similar to the results obtained by Latour *et al.*[30] Compared with the controlled surface without protein adsorption (Fig. 5a), more platelets adhere on the surface with fibrinogen (Fig. 5b) and fibronectin pre-adsorption (Fig. 5c), but a slight increase in the number of adherent platelets on the surface with collagen pre-adsorption (Fig. 5d). Furthermore, the size of adherent platelets on the surfaces with fibrinogen and fibronectin adsorption is much larger than that on the controlled surface and surface with collagen adsorption, indicating the adherent platelets tend to aggregate in the presence of fibrinogen and fibronectin.[34]

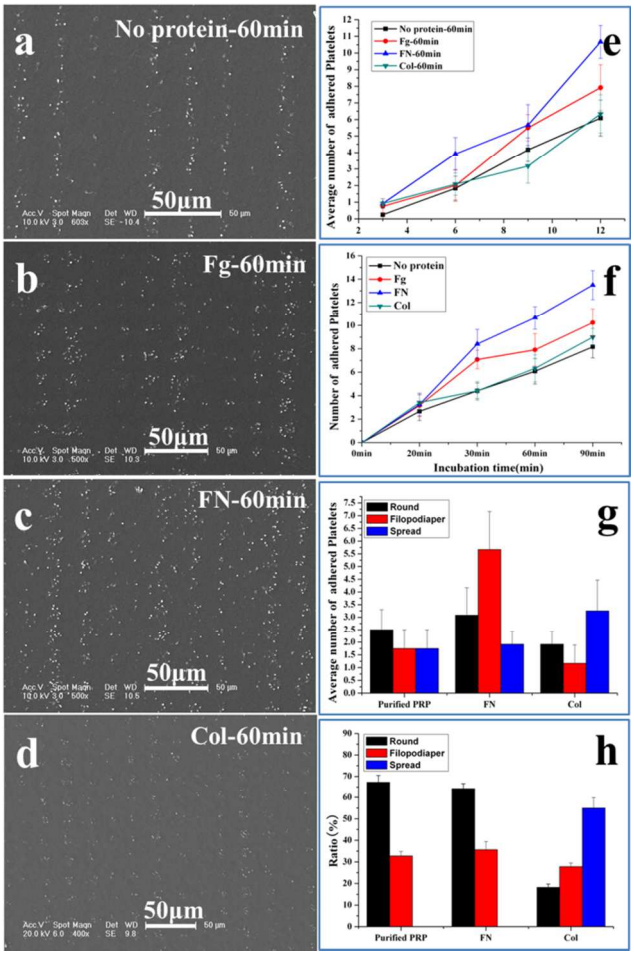

Fig. 5 Adhesion of washed PRP on the patterned surface with adhesive proteins pre-adsorption after 60 min incubation. (a) without adhesive protein pre-adsorption; (b) with fibrinogen (Fg); (c) with fibronectin (FN); (d) with collagen (Col); (e) the number of adherent platelets at varied adhesive sites; (f) time-dependent adhesion at 12 μm adhesive sites; (g), (h) evolution of morphology of adherent platelets at 12 and 3 μm adhesive sites, respectively.

The number of washed platelets at varied adhesive sites is shown in Fig. 5e, at each site, protein adsorption increases the number of adherent platelet, except collagen at 9 μm site. This indicates that collagen has slight effect on the platelet spread.[36] The time dependent occupation of adherent platelets at 12 μm site is shown in Fig. 5f. Initial rate of adhesion with protein adsorption is similar (~0.2 /min), which is double of that without protein adsorption (0.1 /min). The spreading rate without protein adsorption is shown to be about 0.2 /min, but the rates are 0.1, 0.3 and 0.5 /min for collagen, fibrinogen and fibronectin, respectively. The obvious acceleration induced by fibrinogen and fibronectin at spread stage is due to the increased platelet-platelet interactions.[28] Compared with the maximal number of adherent platelets without protein (8.1), the number increases in the order of fibronectin (13.5), fibrinogen (10.3) and collagen (8.3). Fig. 5f supports that collagen has slight effect on the platelet spread while fibronectin and fibrinogen have a similar effect on the platelet adhesion and

spreading.[34] In the following experiments, only fibronectin is used for comparison.

The morphological changes at 12 μm adhesive sites after 60 min incubation are shown in Fig. 5g, without protein adsorption, round shape is slightly higher than filopodiaper and fully spread; when the adhesive sites are adsorbed with fibronectin, the filopodiaper becomes much higher than the round and fully spreading shape; however, when these sites are adsorbed with collagen, the shape of fully spread becomes highest. As round, filopodiaper and fully spread change orderly, high ratio of filopodiaper indicates fibronectin can support more interactions between platelets to form the linkers, while high ratio of fully spread suggests that collagen tends to induce the platelet into compact to stabilize the adhesion.[36]

The role of collagen on platelet adhesion is further confirmed by the morphology of platelets at 3 μm adhesive sites (Fig. 5h). No fully spreading platelets are detected on the sites with fibronectin and without protein due to the confinement. In contrast, the sites with collagen possess high ratio of fully spread, confirming the ability of collagen on stabilization of adhesion in spite of limited space. Our work shows that the response of platelet to adhesive proteins with low concentration (0.1 mg/ml) can be clearly detected. The dominant roles of adhesive proteins on platelets adhesion can thus be distinguished based on the adhesive behaviour on the patterned surface, demonstrating evaluation of platelet function with adhesive behaviour is practical and accurate.

3.4 Evaluation of platelet function based on single platelet adhesion

The antiplatelet and anticancer agents that are widely used to prevent cardiovascular events and tumours will inevitably affect the platelet function.[11, 37] As a consequence, evaluation of platelet function is clinical important to test the toxicity of new agents to platelet. BH3 mimetic are a new class of proapoptotic anticancer agents that have shown considerable promise in preclinical animal models and early-stage human trials.[11] These agents act by inhibiting the prosurvival function of one or more Bcl-2-related proteins. It is well established that these agents can inhibit Bcl-x_L inducing rapid platelet death, resulting in thrombocytopenia. However, their impact on the function of residual circulating platelets remains the issue of debate.[38-40] Some researchers reported these agents that perturb the normal function of mitochondria led to phosphatidylserine (PS) exposure and a procoagulant phenotype,[38] indicating that BH3 mimetics may promote blood coagulation and thrombin generation in vivo.[39] On the contrary, other work showed that BH3 mimetics induced a transient thrombocytopathy that undermined the hemostatic function of platelets.[37, 40] To clarify the effect of BH3 mimetics on the function of platelet, the adhesive behaviour of platelets treated by ABT-737 on the patterned surface are studied.

The SEM images of platelets adherent on patterned surface are shown in Fig. 6. As shown in Fig. 6a-6f, not only the number of adherent platelet decreases with increasing treatment time and dose of ABT-737, but also the pattern of platelets becomes undetectable with high dose and long treatment (eg. 3 μg/ml, 2 h and 6 μg/ml, 2 h). These results confirm that ABT-737 reduces the platelet concentration in a dose and time-dependent manner,[11, 37] but the effect of ABT-737 on platelet function remains unclear because the decrease of platelet concentration leads to the similar incompetence of platelet pattern.

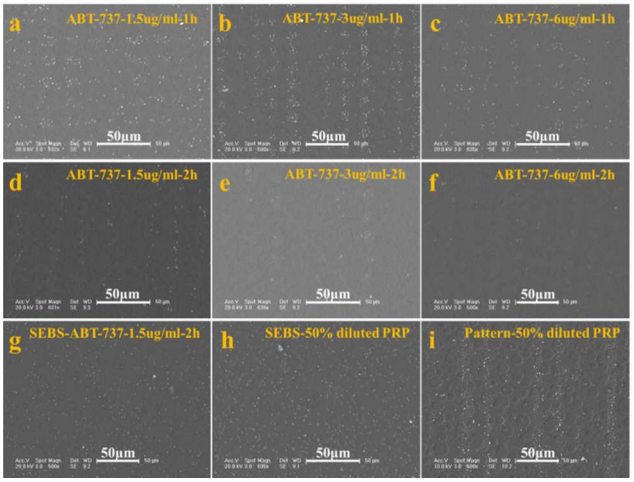

Fig. 6 Adhesion of treated platelets and dilute PRP. (a)-(c) SEM images of adherent platelets after treatments with 1.5 μg/ml, 3 μg/ml and 6 μg/ml ABT-737 for 1 h, respectively; (d)-(f) SEM images of adherent platelets after treatment with 1.5 μg/ml, 3 μg/ml and 6 μg/ml ABT-737 for 2 h, respectively; (g) SEM image of treated platelets (1.5 μg/ml, 2 h) adherent on blank film. (h), (i). SEM images of dilute PRP (50%) adherent on blank film and patterned surface, respectively. Based on the adhesive behaviour on patterned surfaces, it is confirmed that ABT-737 induces not only decreased platelet number but also reduced adhesive ability of platelet.

According to the number of adherent platelet on the blank surface without pattern, the concentration of lived platelets is estimated to be about 50 % concentration of PRP after PRP is treated with 1.5 μg/ml ABT-737 for 2 h (Support Information Fig. S5). The adhesion of treated platelets (1.5 μg/ml, 2 h) and diluted PRP (50%) are thus performed on a blank film and patterned surface, respectively, to clarify the effect of ABT-737 on platelet function.

The slight differences are observed in morphology and adherent number between adhesion on the blank surfaces with treated PRP (Fig. 6g) and with dilute PRP (Fig. 6h). In contrast, the obvious distinctions on the platelet pattern on the patterned surfaces treated PRP (Fig. 6d) and with diluted PRP (Fig. 6i) are detected, and the pattern of adherent platelets of diluted PRP is much clearer than the pattern of treated platelets, showing the advantage of patterned surface in detection.[15] The average numbers of adherent platelets treated by ABT-737 at 3 and 12 μm are about 1/2 and 1/3 of number of diluted platelets adherent at 3 and 12 μm, respectively, confirming that ABT-737 induces not only decreased platelet number (thrombocytopenia) but also reduced adhesive ability.[37] Based on the single platelet adhesion on the patterned surface, our research successfully assess platelet function in the presence of antiplatelet agents, which provides a new avenue for accurate

detection of dysfunctional platelet and drug effects in cancer patients.[41]

Conclusions

In this work, we have developed a facile and stable UV lithography technique combined with a photomask to achieve physical adhesive sites in the range from 12 μm to 3 μm on the patterned surface of SEBS. With the simplicity and effectiveness of patterned surface, single platelet adhesion was controlled and quantitatively probed. Patterned surface rendered adhesion sensitive to adhesive proteins and enabled assessment of platelet function through single platelet adhesion. Our work paves a new way to understand and evaluate the platelet function both in research and clinical diagnostics. The methodology has the potential to enable a rapid, accurate point-of-care platform suitable to evaluation of platelet function, detection of dysfunctional platelets and the administration of antiplatelet agents.

Acknowledgements

The authors acknowledge the financial support of the National Natural Science Foundation of China (Project No. 51273199, 21274150 and 51103030).

Notes and references

[a] Polymer Physics and Chemistry, Changchun Institute of Applied Chemistry, Chinese Academy of Sciences, Changchun, 130022, China.
[b] Department of Mechanical Engineering, University of Akron, Akron, Ohio 44325-3903, USA.
[c] Polymer Materials Research Center and Key Laboratory of Superlight Materials and Surface Technology, Ministry of Education, College of Materials Science and Chemical Engineering, Harbin Engineering University, Harbin 150001, China.

Electronic Supplementary Information (ESI) available: [details of any supplementary information available should be included here]. See DOI: 10.1039/b000000x/

1 M. Leslie, *Science*, 2010, **328**, 562-564.
2 C. R. Engwerda and M. F. Good, *Science*, 2012, **338**, 1304-1305.
3 G. A. Zimmerman and A. S. Weyrich, *Science*, 2010, **327**, 528-529.
4 S. Vaiyapuri, L. A. Moraes, T. Sage, M. S. Ali, K. R. Lewis, M. P. Mahaut-Smith, E. Oviedo-Orta, A. M. Simon and J. M. Gibbins, *Nat. Commun.*, 2013, **4**.
5 K. M. Hoffmeister, E. C. Josefsson, N. A. Isaac, H. Clausen, J. H. Hartwig and T. P. Stossel, *Science*, 2003, **301**, 1531-1534.
6 K. D. Mason, M. R. Carpinelli, J. I. Fletcher, J. E. Collinge, A. A. Hilton, S. Ellis, P. N. Kelly, P. G. Ekert, D. Metcalf and A. W. Roberts, *Cell*, 2007, **128**, 1173-1186.
7 Lopez-Alonso, A.; Jose, B.; Somers, M.; Egan, K.; Foley, D. P.; Ricco, A. J.; Ramström, S.; Basabe-Desmonts, L.; Kenny, D. *Anal. Chem.*, 2013, ***85***, 6497-6504.
8 Z. M. Ruggeri and G. L. Mendolicchio, *Circ. Res.*, 2007, **100**, 1673-1685.
9 T. Ekblad, L. Faxälv, O. Andersson, N. Wallmark, A. Larsson, T. L. Lindahl and B. Liedberg, *Adv. Funct. Mater.*, 2010, **20**, 2396-2403.
10 L. Brass, *ASH Education Program Book*, 2010, **2010**, 387-396.
11 B. Savage, E. Saldívar and Z. M. Ruggeri, *Cell*, 1996, **84**, 289-297.
12 L. Brass, in. *Platelets*, ed. A. Michelson. Academic press, London, **2007**. p. 367-398.
13 Z. Li, E. S. Kim and E. L. Bearer, *Blood*, 2002, **99**, 4466-4474.
14 L. Basabe-Desmonts, S. Ramstrom, G. Meade, S. O'neill, A. Riaz, L. Lee, A. Ricco and D. Kenny, *Langmuir*, 2010, **26**, 14700-14706.
15 W. Ye, Q. Shi, S. C. Wong, J. Hou, H. Shi and J. Yin, *Macromol. Biosci.,* 2013, **13**, 676-681.
16 C. Choi, I. Hwang, Y.-L. Cho, S. Y. Han, D. H. Jo, D. Jung, D. W. Moon, E. J. Kim, C. S. Jeon and J. H. Kim, *ACS Appl. Mater. Interfaces*, 2013, **5**, 697-702.
17 A. Kita, Y. Sakurai, D. R. Myers, R. Rounsevell, J. N. Huang, T. J. Seok, K. Yu, M. C. Wu, D. A. Fletcher and W. A. Lam, *PloS one*, 2011, **6**, e26437.
18 Zhu, X.; Jańczewski, D.; Lee, S.S.C.; Teo, S.L.; Vancso, G. J. *ACS Appl. Mater. Interfaces,* **2013**, *5*, 5961-5968.
19 L. E. Corum, C. D. Eichinger, T. W. Hsiao and V. Hlady, *Langmuir*, 2011, **27**, 8316-8322.
20 M. J. Price, S. Endemann, R. R. Gollapudi, R. Valencia, C. T. Stinis, J. P. Levisay, A. Ernst, N. S. Sawhney, R. A. Schatz and P. S. Teirstein, *Eur. Heart. J.*, 2008, **29**, 992-1000.
21 J. Hou, Q. Shi, P. Stagnaro, W. Ye, J. Jin, L. Conzatti and J. Yin, *Colloid. Surface. B*, 2013, **111**, 333-341.
22 T. Konno, H. Hasuda, K. Ishihara and Y. Ito, *Biomaterials*, 2005, **26**, 1381-1388.
23 M. R. Lorenz, V. Holzapfel, A. Musyanovych, K. Nothelfer, P. Walther, H. Frank, K. Landfester, H. Schrezenmeier and V. Mailänder, *Biomaterials*, 2006, **27**, 2820-2828.
24 Z. M. Ruggeri, J. N. Orje, R. Habermann, A. B. Federici and A. J. Reininger, *Blood*, 2006, **108**, 1903-1910.
25 C. S. Chen, M. Mrksich, S. Huang, G. M. Whitesides and D. E. Ingber, *Science*, 1997, **276**, 1425-1428.
26 J. Zhao, L. Song, Q. Shi, S. Luan and J. Yin, *ACS Appl. Mater. Interfaces,* 2013, **5**, 5260-5268.
27 C. Yan, J. Sun and J. Ding, *Biomaterials*, 2011, **32**, 3931-3938.
28 M. J. Maxwell, E. Westein, W. S. Nesbitt, S. Giuliano, S. M. Dopheide and S. P. Jackson, *Blood*, 2007, **109**, 566-576.
29 C. H. Jo, J. E. Kim, K. S. Yoon and S. Shin, *Am. J. Sport. Med.*, 2012, **40**, 1035-1045.
30 B. Sivaraman and R. A. Latour, *Biomaterials*, 2010, **31**, 832-839.
31 P. K. Mattila and P. Lappalainen, *Nat. Rev. Mol. Cell. Bio.*, 2008, **9**, 446-454.
32 W. A. Lam, O. Chaudhuri, A. Crow, K. D. Webster, A. Kita, J. Huang and D. A. Fletcher, *Nat. Mater.*, 2010, **10**, 61-66.
33 S. Beumer, M. IJsseldijk, P. G. de Groot and J. J. Sixma, *Blood*, 1994, **84**, 3724-3733.
34 T. Zaidi, L. McIntire, D. Farrell and P. Thiagarajan, *Blood*, 1996, **88**, 2967-2972.
35 E. Saelman, H. K. Nieuwenhuis, K. M. Hese, P. G. de Groot, H. Heijnen, E. Sage, S. Williams, L. McKeown, H. Gralnick and J. Sixma, *Blood*, 1994, **83**, 1244-1250.
35 B. Nieswandt and S. P. Watson, *Blood*, 2003, **102**, 449-461.

37 S. M. Schoenwaelder, K. E. Jarman, E. E. Gardiner, J. Qiao, M. J. White, E. C. Josefsson, I. Alwis, A. Ono, A. Willcox and R. K. Andrews, *Blood*, 2011, **118**, 1663-1674.
38 G. Dale, *J. Thromb. Haemost.*, 2005, **3**, 2185-2192.
39 S. M. Schoenwaelder, Y. Yuan, E. C. Josefsson, M. J. White, Y. Yao, K. D. Mason, L. A. O'Reilly, K. J. Henley, A. Ono and S. Hsiao, *Blood*, 2009, **114**, 663-666.
40 S. M. Schoenwaelder and S. P. Jackson, *Blood*, 2012, **119**, 1320-1321.
41 L. J. Gay and B. Felding-Habermann, *Nat. Rev. Cancer*, 2011, **11**, 123-134.